

Sphingosine-1-phosphate Phosphatase 1 Regulates Keratinocyte Differentiation and Epidermal Homeostasis^{*S}

Received for publication, April 17, 2013 Published, JBC Papers in Press, May 1, 2013, DOI 10.1074/jbc.M113.478420

Maria L. Allende, Laura M. Sipe, Galina Tuymetova, Kelsey L. Wilson-Henjum, Weiping Chen, and Richard L. Proia¹

From the Genetics of Development and Disease Branch, NIDDK, National Institutes of Health, Bethesda, Maryland 20892

Background: Sphingosine-1-phosphate phosphatase 1, encoded by *Sgpp1*, dephosphorylates the signaling lysophospholipid, S1P; however, its *in vivo* functions are not well understood.

Results: Deletion of *Sgpp1* causes epidermal defects with intrinsic keratinocyte abnormalities.

Conclusion: *Sgpp1* deficiency in keratinocytes causes S1P elevation and accelerates their differentiation.

Significance: Intracellular S1P metabolism regulates keratinocyte differentiation and epidermal homeostasis.

Sphingosine 1-phosphate (S1P) is a bioactive lipid whose levels are tightly regulated by its synthesis and degradation. Intracellularly, S1P is dephosphorylated by the actions of two S1P-specific phosphatases, sphingosine-1-phosphate phosphatases 1 and 2. To identify the physiological functions of S1P phosphatase 1, we have studied mice with its gene, *Sgpp1*, deleted. *Sgpp1*^{−/−} mice appeared normal at birth, but during the 1st week of life they exhibited stunted growth and suffered desquamation, with most dying before weaning. Both *Sgpp1*^{−/−} pups and surviving adults exhibited multiple epidermal abnormalities. Interestingly, the epidermal permeability barrier developed normally during embryogenesis in *Sgpp1*^{−/−} mice. Keratinocytes isolated from the skin of *Sgpp1*^{−/−} pups had increased intracellular S1P levels and displayed a gene expression profile that indicated overexpression of genes associated with keratinocyte differentiation. The results reveal S1P metabolism as a regulator of keratinocyte differentiation and epidermal homeostasis.

Sphingosine 1-phosphate (S1P)² is a bioactive lipid that directly participates in both intracellular and extracellular signaling (1–4). Among the first signaling activities identified for S1P was its intracellular action to mobilize Ca²⁺ from internal stores (5, 6). More recently, several other intracellular targets have been identified (7, 8). Extracellular S1P exerts its effects through interactions with the family of S1P G protein-coupled receptors (S1PR1–5) that are carried by most cells, either singly or in different combinations. These receptors trigger distinctive cellular signaling pathways and exert control within the

immune, vascular, and nervous systems (1–3). In addition to its important role in cellular signaling, S1P also functions as a key intermediate in lipid metabolic pathways (9).

S1P levels are tightly controlled by the regulation of its synthesis and degradation (see *scheme* in Fig. 1A) (10). After the formation of ceramide by *de novo* synthesis or degradation of complex sphingolipids, sphingosine is liberated by the action of ceramidase. S1P is then synthesized via the ATP-dependent phosphorylation of sphingosine by the sphingosine kinases, Sphk1 or Sphk2. Intracellularly, S1P is degraded in either of two ways, through dephosphorylation by the S1P phosphatases (SPP) SPP1 and SPP2 to yield sphingosine or through irreversible cleavage by S1P lyase. Extracellularly, S1P is dephosphorylated by the lipid phosphate phosphatases (LPP) LPP1, LPP2, and LPP3.

Both the SPPs and LPPs are members of the superfamily of phosphohydrolases (11–14). SPPs are highly specific for sphingoid-base 1-phosphate substrates, including S1P, dihydro-S1P, and phyto-S1P (15), whereas LPPs have a broader specificity that includes S1P but also ceramide 1-phosphate, lysophosphatidic acid, and phosphatidic acid. SPPs are integral enzymes of the endoplasmic reticulum (ER) (16–19) with a luminal active site. In contrast, the LPPs are found on the plasma membrane with their active site oriented to the cell exterior (11, 20). Their localization suggests that SPPs and LPPs have distinct pools of S1P as substrate, with the SPPs dephosphorylating intracellular S1P, and the LPPs dephosphorylating S1P in the extracellular space. Indeed, deletion of LPP3 blocked the egress of lymphocytes from the thymus, an important extracellular signaling function of S1P, supporting the notion that LPPs are ectoenzymes that regulate extracellular levels of S1P for signaling (20).

Within the sphingolipid metabolic pathway, SPP activity has been shown to influence the levels of both S1P and ceramide, presumably by diverting the sphingoid-base substrate from S1P formation back to ceramide synthesis. Functionally, the SPPs have been shown to have diverse cellular activities. SPP1 has been shown to regulate apoptosis by elevating ceramide levels (15), ER-to-Golgi ceramide trafficking (21), and autophagy induced by ER stress (22, 23). In addition, its effects on S1P levels influence resistance artery tone (24) and cell migration (25). SPP2 has been found to be elevated during immune responses (26). However, despite being implicated in diverse

^{*} This work was supported, in whole or in part, by National Institutes of Health grants from NIDDK, Grant P30 CA138313 (to Lipidomics Shared Resource, Hollings Cancer Center, Medical University of South Carolina), and Grant P20 RR017677 (to Lipidomics Core in the South Carolina Lipidomics and Pathobiology COBRE).

[†] This article was selected as a Paper of the Week.

[§] This article contains supplemental Figs. S1–S5 and Table S1.

¹ To whom correspondence should be addressed: Genetics of Development and Disease Branch, NIDDK, Bldg. 10, Rm. 9D-06, 10 Center Dr. MSC 1821, Bethesda, MD 20892-1821. E-mail: rp36y@nih.gov.

² The abbreviations used are: S1P, sphingosine 1-phosphate; SPP, sphingosine-1-phosphate phosphatase; LPP, lipid phosphate phosphatase; ER, endoplasmic reticulum; RT-qPCR, real time-quantitative PCR; E, embryonic day.

Sgpp1 and Keratinocyte Differentiation

activities, the roles of the SPPs in physiology are not well understood.

Sphingolipids are recognized for their importance in skin biology as both structural and signaling molecules (27–30). Recently, S1P has been shown to have signaling properties that regulate keratinocyte cell function (31–36). Here, we report that the deletion of *Sgpp1*, the gene encoding SPP1, greatly disturbs epidermal homeostasis in mice. Keratinocytes lacking *Sgpp1* have elevated S1P levels and overexpress genes associated with differentiation. These results link *Sgpp1* expression with skin biology through the regulation of keratinocyte differentiation by S1P metabolism.

EXPERIMENTAL PROCEDURES

Mouse Generation and Procedures—*Sgpp1*^{−/−} mice were generated by the Knock-out Mouse Project Repository (University of California, Davis) from ES cells created by Velocigene Regeneron Pharmaceuticals, Inc. (Tarrytown, NY). The mice had a C57Bl6 background and were maintained by heterozygous mating. Mice were genotyped by multiplex PCR of tail-snip DNA using three primers as follows: 5′-CGTGTTCATGACATTCGCCAAGC-3′ (F1); 5′-GGAAATGGCTCCCAGAGGAAA-3′ (F2); and 5′-GCACCTCTGTTCCACATACAC-3′ (R) (Fig. 1B). The following conditions were used: denaturation, 94 °C for 5 min; amplification, 94 °C for 1 min, 60 °C for 1 min, 72 °C for 1.5 min; and extension, 72 °C for 3 min (35 cycles). The WT *Sgpp1* gene fragment was 588 bp in length, and the mutant *Sgpp1* gene fragment was 402 bp in length.

Pups were analyzed at days 1 or 2 after birth, unless otherwise specified. Adult *Sgpp1*^{−/−} mice were analyzed when they were between 7 and 10 months old. Littermate WT (*Sgpp1*^{+/+}) mice were used as controls for each experiment. All animal procedures were approved by the NIDDK Animal Care and Use Committee and were performed in accordance with National Institutes of Health guidelines.

Histology and Immunohistochemistry—Skin tissue from *Sgpp1*^{+/+} and *Sgpp1*^{−/−} mice was fixed with 10% formalin and embedded in paraffin. Sections were stained with H&E and examined on a Leica DMLB microscope (Leica Microsystems Inc., Buffalo Grove, IL). The epidermis was divided into two regions as follows: the stratum corneum, which is the top flaky layers stained by eosin and characterized by the lack of nuclei; and the subcorneal layers, right below the stratum corneum, which included the rest of the epidermis (from the top: stratum granulosum, stratum spinosum, and stratum basale) and were distinguished by hematoxylin staining. Quantification of epidermal thickness was done on photographs acquired from H&E-stained sections with a ×10 objective, using the image analysis program ImageJ. A scale was made within ImageJ from an ocular ruler photographed using the same microscopic field as the skin sections. Ten perpendicular lines were drawn from the bottom edge of the subcorneal layers to the top edge of the stratum corneum. The mean length of the lines was determined for two photographs/mouse.

For immunostaining, deparaffinized sections of back skin from pups and adult mice were incubated separately with the following antibodies: rabbit anti-mouse keratin 6 (PRB-169P-100); keratin 10 (PRB-159P-100); keratin 14 (PRB-155P-100);

loricrin (PRB-145P-100); filaggrin (PRB-417P-100) (all from Covance, Philadelphia, PA); and Ki67 antigen (ab66155; from Abcam, Cambridge, MA), followed by Alexa Fluor 488-conjugated goat anti-rabbit IgG secondary antibody (A11034; from Invitrogen) and DAPI. Sections were examined using a confocal laser scanning microscope with a Duo-Scan system (LSM 5 LIVE; Carl Zeiss, Inc., Thornwood, NY) using a ×20 objective. Excitation and filters were as follows: Alexa Fluor 488, laser 489 nm for excitation, emission collected with BP 520–555-nm filter; and DAPI, laser 405 nm for excitation, emission collected with BP 415–480-nm filter. Images were acquired using the ZEN 2007 software (Carl Zeiss, Inc.).

β-Galactosidase expression from the *lacZ* reporter was determined on the back skin of 2-day-old *Sgpp1*^{+/+} mice using 5-bromo-4-chloro-3-indolyl-β-D-galactoside (X-gal) as described previously (37). *Sgpp1*^{+/+} skin sections were used as negative control.

Determination of Ca²⁺ Distribution in Situ in Mouse Skin—Ca²⁺ distribution was detected in intact frozen skin sections obtained from 4-day-old pups as described previously (33, 38). Briefly, a 10-μm frozen skin section was placed on a glass slide covered by a thin layer of 2% agarose containing 10 μg/ml Calcium Green-1 (Invitrogen). Sections were observed using a Leica DMLB microscope within the next 2 h.

Primary Keratinocyte Cultures—Primary keratinocyte cultures were prepared as described previously (39, 40). Briefly, skin was removed from 1-day-old pups and placed in 0.25% trypsin without EDTA overnight at 4 °C. The epidermis was peeled away from the dermis with forceps, then minced, and filtered. Cells were plated on collagen-coated plates. Using this protocol, only keratinocytes from the stratum basale attach to the plates. Keratinocytes were grown in 0.05 mM Ca²⁺-containing Eagle's minimum essential medium (Lonza, Walkersville, MD) plus 8% fetal calf serum (low Ca²⁺ medium) for 3–4 days and then harvested. Alternatively, WT mouse keratinocytes were obtained from (CELLnTEC Advance Cell Systems, Bern, Switzerland) and were grown in CnT7 medium containing 0.07 mM Ca²⁺ (CELLnTEC Advance Cell Systems).

When indicated, WT keratinocytes were treated with 10^{−7} M S1P (Avanti Polar Lipids, Inc., Alabaster AL) for 2 days in CnT2 medium (CELLnTEC Advance Cell Systems) containing 1.2 mM Ca²⁺. Conditioned medium from 5-day-old *Sgpp1*^{+/+} and *Sgpp1*^{−/−} keratinocyte cultures grown in CnT7 medium were collected and centrifuged at 200 × g for 10 min.

Lipid Analysis—Skin dissected from the back of 2-day-old *Sgpp1*^{+/+} and *Sgpp1*^{−/−} mice was placed on top of calcium/magnesium-free PBS containing 10 mM EDTA (pH 7.4) with the dermal side facing downward. After incubating for 40 min at 37 °C, the epidermis was peeled away from the dermis with forceps (41). Epidermal sheets were quickly rinsed with normal saline and frozen at −80 °C. Keratinocytes growing in culture were washed, harvested, and cell pellets frozen at −80 °C. Plasma was prepared from blood from adult *Sgpp1*^{+/+} and *Sgpp1*^{−/−} mice. Sphingolipids were extracted from the epidermal sheets, keratinocyte pellets, and plasma, and S1P, dihydro-S1P, sphingosine, and ceramides containing different nonhydroxy amide-linked fatty acid species were measured by HPLC-tandem MS by the Lipidomics Core at the Medical University of

South Carolina on a Thermo Finnigan (Waltham, MA) TSQ 7000 triple quadrupole mass spectrometer, operating in a multiple reaction-monitoring positive ionization mode as described previously (42). Sphingolipid concentration was normalized using inorganic phosphate measurements of the lipid extracts.

For sphingomyelin determinations, lipid extracts were prepared from epidermis and keratinocyte pellets as described previously (43), applied to high performance thin layer chromatography (HPTLC) plates (Merck), and developed in chloroform/methanol/water (65:35:8). After running, HPTLC plates were sprayed with 1.5% cupric sulfate in acetic acid/sulfuric acid/orthophosphoric acid/water (50:10:10:30) and baked at 110 °C for 10 min. Bands were identified using known standards run simultaneously with the samples and quantified using the Carestream Molecular Imaging Software (Carestream Health, Inc., Rochester, NY). Sphingomyelin concentrations were normalized using inorganic phosphate measurements of the lipid extracts.

S1P-induced Down-modulation of S1PR1-GFP Receptor from the Plasma Membrane—HEK293 cells stably expressing the S1PR1-GFP chimeric receptor (44) were grown in 10% charcoal-stripped FBS-containing DMEM (C-DMEM) for 24 h and treated for 60 min with 10^{-7} M S1P, 5-day *Sgpp1*^{+/+} and *Sgpp1*^{-/-} keratinocyte-conditioned medium, or C-DMEM alone. Cells were then fixed with 1% paraformaldehyde in PBS for 15 min and examined for GFP and DAPI using a Zeiss confocal laser scanning microscope under a $\times 63$ oil objective.

Skin Permeability Assays—Embryos obtained by Caesarean section at days 16.5 and 17.5 postcoitum (which was determined by the presence of a vaginal plug at day 0.5) and 4-day-old pups were euthanized. Mice were fixed in methanol for 5 min at room temperature, washed five times with PBS, and incubated with 0.1% toluidine blue in normal saline for 10 min (41). After washing with PBS, mice were examined for the penetration of the blue dye into the skin and photographed.

Gene Expression—Total RNA from mouse tissues was purified using TRIzol (Invitrogen) and from keratinocyte cultures cells using the RNeasy mini kit (Qiagen, Valencia, CA). Total RNA (1 μ g) was first digested with DNase I and subsequently reverse-transcribed with the SuperScript First-Strand Synthesis System (Invitrogen) by following the manufacturer's instructions.

For semiquantitative RT-PCR, the forward primer (rt1, 5'-tatcggaatgcattctat-3') was located on exon 1 of the *Sgpp1* transcript, and the reverse primer (rt2, 5'-GCTTTTCCAAACAGAGTTACA-3') was located on exon 3 (Fig. 1B). The following conditions were used: denaturation, 95 °C for 5 min; amplification, 95 °C for 1 min, 55 °C for 1 min, 72 °C for 1 min; and extension, 72 °C for 3 min (35 cycles). For amplification of *Gapdh* mRNA, the forward primer was at the exon 4–5 junction (5'-ACCACAGTCCATGCCATCAC-3') and the reverse primer was in exon 7 (5'-CACCACCCTGTTGCTGTAGCC-3'). The following conditions were used: denaturation, 95 °C for 5 min; amplification, 95 °C for 1 min, 65 °C for 1 min, 72 °C for 1 min; and extension, 72 °C for 3 min (35 cycles). PCR products were visualized on a 1.2% agarose gel.

Alternatively, mRNA expression levels were determined by real time-quantitative PCR (RT-qPCR) using pre-designed Assay-on-Demand probes and primers (Applied Biosystems, Foster City, CA) on an ABI Prism 7700 Sequence Detection System (Applied Biosystems) as follows: for mouse *Sgpp1* (Mm00473016_m1); *Sgpp2* (Mm01158866_m1); *Sgpl1* (Mm00486079_m1); *Flg* (Mm01716522_m1); *Lor* (Mm01219285_m1); *Krt10* (Mm03009921_m1); *Krt14* (Mm00516876_m1); *Lce1c* (Mm00783426_s1); *Rptn* (Mm00485857_m1); *Tgm3* (Mm00436999_m1); *Cdsn* (Mm01275230_m1); *Lor* (Mm01962650_s1); *Hrnr* (Mm00808280_s1); *Spink5* (Mm00511522_m1); *Ppap2a* (Mm00477016_m1); *Ppap2b* (Mm005404516_m1); *Ppap2c* (Mm00479290_m1), and *Gapdh* (Mm99999915_g1).

For microarray analysis, total RNA purified from primary keratinocyte cultures of *Sgpp1*^{+/+} and *Sgpp1*^{-/-} cells was analyzed on Affymetrix GeneChip Mouse Genome 430 2.0 arrays (Affymetrix, Santa Clara, CA) as described previously (9). The National Center for Biotechnology Information Gene Expression Omnibus (GEO) accession number for the microarray data is GSE40838.

Statistical Analysis—Statistical significance was determined using the Student's *t* test. In all cases, *p* < 0.05 was considered statistically significant.

RESULTS

***Sgpp1* Deficiency Results in Neonatal Lethality and Abnormal Skin in Newborn Pups**—The structure of the targeted *Sgpp1* allele mouse is shown in Fig. 1B. The targeting vector replaced the entire *Sgpp1* coding region, beginning at the start codon in exon 1 and extending into exon 3, with *lacZ* and *neo* cassettes (Fig. 1B). This targeting procedure is expected to result in a null *Sgpp1* allele and a *lacZ* reporter under the control of the native *Sgpp1* promoter elements.

Expression of *Sgpp1* was readily detectable in tissues of *Sgpp1*^{+/+} mice by semiquantitative RT-PCR (Fig. 1, C and D) and RT-qPCR (Fig. 1, E and F), but it was below the level of detection in *Sgpp1*^{-/-} mice, confirming that the gene targeting procedure had successfully generated a null *Sgpp1* allele. Expression levels of *Sgpp2*, the gene encoding the second SPP isozyme, were not significantly altered in *Sgpp1*^{-/-} mouse tissues (Fig. 1F).

Sgpp1^{+/-} mice were bred, and offspring were genotyped at a few days after birth or at 3 weeks of age. Newborn *Sgpp1*^{-/-} pups were found in a Mendelian ratio (from a total of 182 pups, 26% were *Sgpp1*^{+/+}, 51% *Sgpp1*^{+/-}, and 23% *Sgpp1*^{-/-}). However, only 3.5% of the offspring were *Sgpp1*^{-/-} when they were weaned at 3 weeks of age. These results indicated that a substantial fraction of the *Sgpp1*^{-/-} mice died between birth and 3 weeks of age.

Immediately after birth, *Sgpp1*^{-/-} pups could not be distinguished from *Sgpp1*^{+/+} littermates (Fig. 2A). However, starting at 3 days of age, *Sgpp1*^{-/-} mice appeared smaller than their littermates. In addition, they showed skin desquamation on the trunk and around the joints of the upper and lower extremities that progressively worsened with time (Fig. 2B). Skin sections from 2-day-old pups showed that *Sgpp1*^{-/-} epidermis was thickened compared with WT epidermis (Fig. 2, C and D). His-

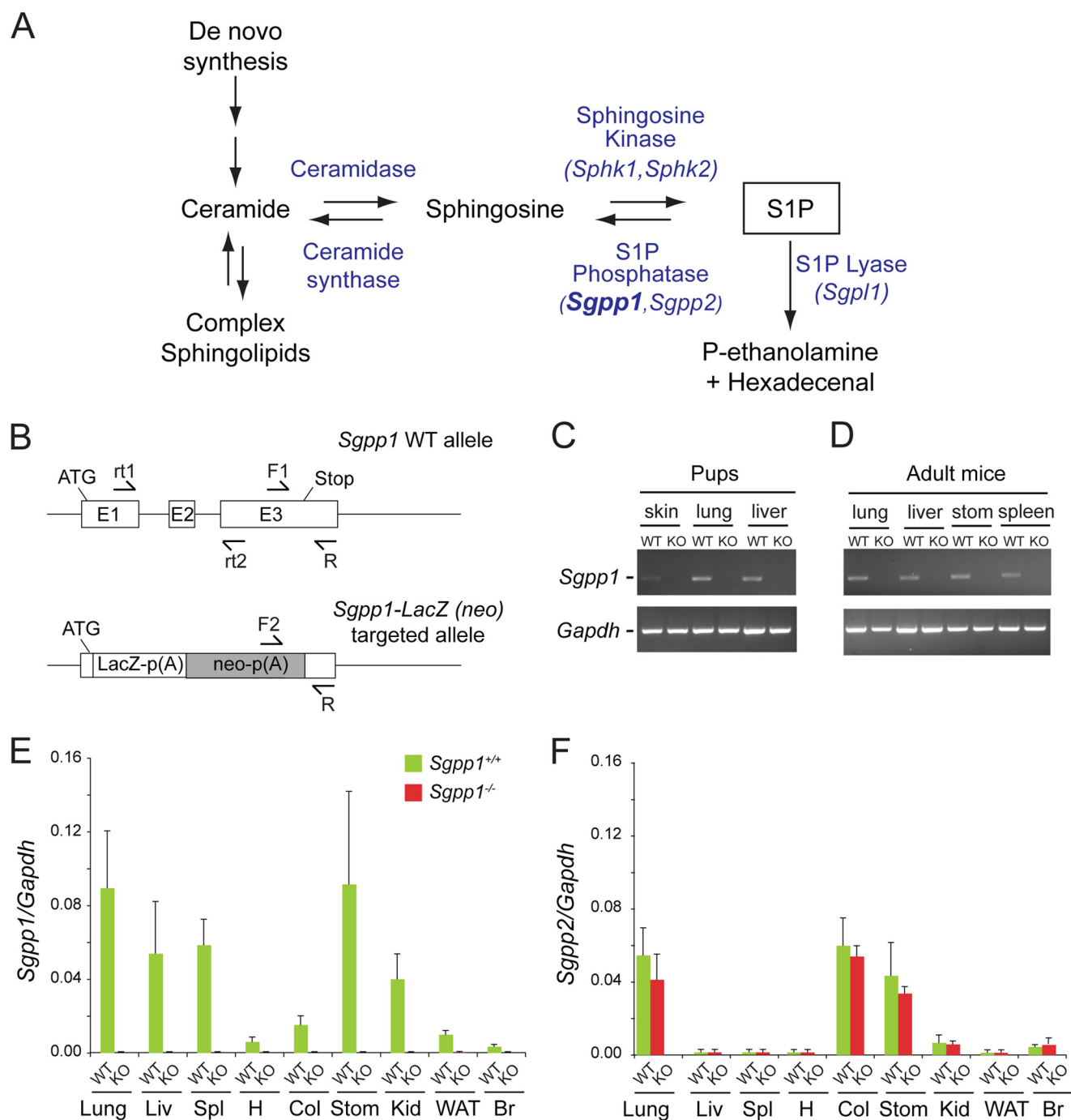


FIGURE 1. Generation of *Sgpp1* knock-out mouse line by *Sgpp1* gene disruption. A, intracellular metabolic pathway of S1P. B, schematic representation of the *Sgpp1* gene targeting strategy. The structure of the mouse *Sgpp1* locus is shown at the top, and the structure of the *Sgpp1* targeted allele is shown at the bottom. Arrows F1, F2, and R represent the primers used for genotyping; arrows rt1 and rt2 represent the primers used in semiquantitative RT-PCR. C and D, mRNA expression for *Sgpp1* (top gels) and *Gapdh* (bottom gels) determined by semiquantitative RT-PCR of various tissues from *Sgpp1*^{+/+} (WT) and *Sgpp1*^{-/-} (KO) 2-day-old (C) and adult (D) mice. E and F, mRNA expression for *Sgpp1* (E) and *Sgpp2* (F) determined by RT-qPCR of various tissues from *Sgpp1*^{+/+} and *Sgpp1*^{-/-} adult mice. Liv, liver; Spl, spleen; H, heart; Col, colon; Stom, stomach; Kid, kidney; WAT, white adipose tissue; Br, brain. The relative level of *Gapdh* mRNA expression in each sample was set to 1. Bars represent mean values ± S.D. Student's *t* test, *n* = 4.

tological analysis of *Sgpp1*^{-/-} back skin undergoing peeling showed the detachment of the stratum corneum (Fig. 2E). Measurements demonstrated that, in *Sgpp1*^{-/-} mice, the subcorneal layers (which included the stratum granulosum, stratum spinosum, and stratum basale) were significantly thicker, whereas the stratum corneum was thinner than in *Sgpp1*^{+/+} mice (Fig. 2F). These results indicate that the deletion of the *Sgpp1* gene induces epidermal abnormalities in newborn mice.

Expression of *Sgpp1* in Epidermis—The expression of *Sgpp1* in the epidermis was determined using a surrogate marker, β -galactosidase, the product of the *lacZ* gene, which had been placed under the control of the native *Sgpp1* regulatory elements in the *Sgpp1* gene-targeted mice (see targeting scheme in Fig. 1B). In skin sections from 2-day-old *Sgpp1*^{+/+} mice stained for β -galactosidase activity, intense blue reaction product was observed in the stratum granulosum and the stratum spinosum

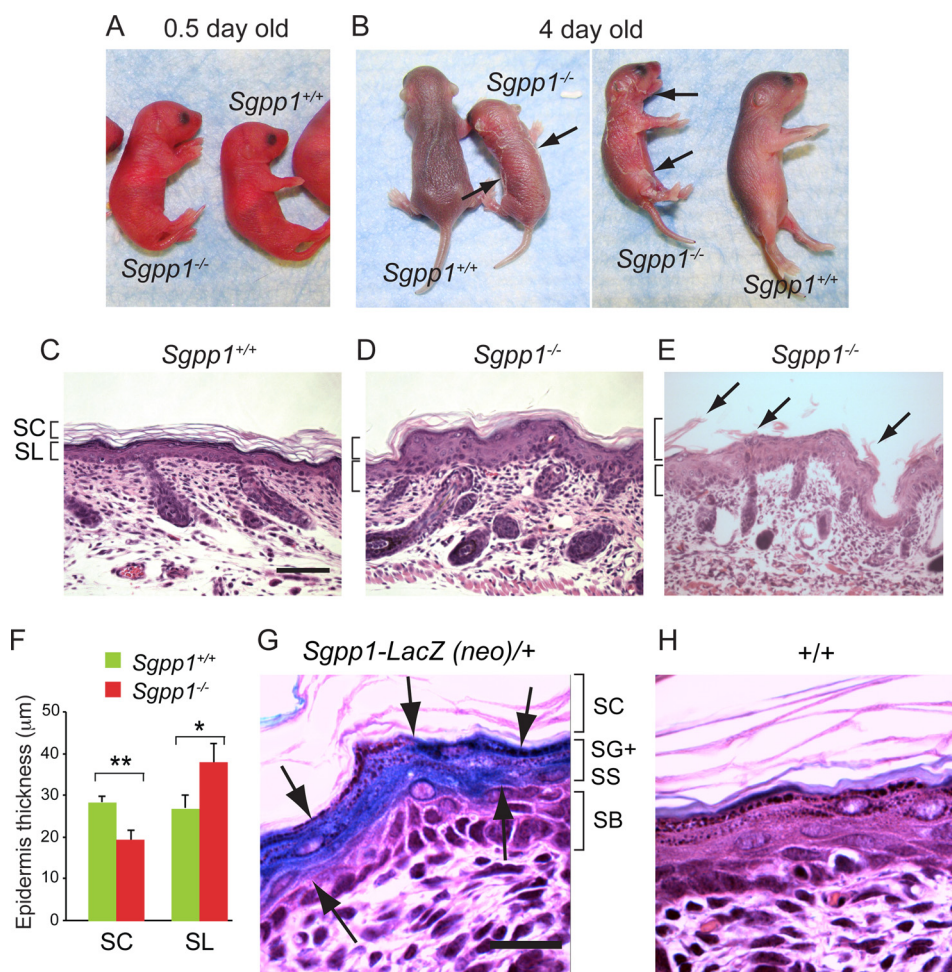


FIGURE 2. *Sgpp1*^{-/-} pups exhibit focal desquamation and abnormal epidermal histology. A and B, *Sgpp1*^{+/+} and *Sgpp1*^{-/-} mice at 0.5 days (A) and 4 days after birth (B). The arrows in B indicate sites of desquamation. C–E, histology of *Sgpp1*-deficient mouse skin. Paraffin sections of back skin from 2-day-old *Sgpp1*^{+/+} (C) and *Sgpp1*^{-/-} (D and E) mice were stained with H&E. E represents a region of back skin undergoing peeling of the stratum corneum (marked by arrows). Bar, 200 μm. SC, stratum corneum; SL, subcorneal layer. F, stratum corneum and subcorneal layer thicknesses in 2-day-old *Sgpp1*^{+/+} and *Sgpp1*^{-/-} mice. Bars represent mean values ± S.D. *n* = 4 for each genotype. Student's *t* test; *, *p* < 0.05; **, *p* < 0.01. G and H, activity of β-galactosidase, a surrogate marker for *Sgpp1* expression, in 2-day-old mouse skin section. *Sgpp1*^{+/+} (*Sgpp1*-LacZ (neo)/+) (G) and *Sgpp1*^{+/+} (+/+) (H) skin sections are shown. Arrows in G mark the keratinocyte layers that express β-galactosidase as a marker of *Sgpp1* expression. This staining is absent in the +/+ skin section (H). Bar, 50 μm. SC, stratum corneum; SG, stratum granulosum; SS, stratum spinosum; SB, stratum basale.

(Fig. 2G). *Sgpp1*^{+/+} skin sections without the *lacZ* reporter were largely negative for β-galactosidase activity (Fig. 2H). This result suggests that the expression of the *Sgpp1* gene is up-regulated as keratinocytes differentiate within the epidermis.

We also determined the relative mRNA expression of the three specific S1P degradation enzymes, the two SPPs (*Sgpp1* and *Sgpp2*) and S1P lyase (*Sgpl1*), in the skin of 2-day-old *Sgpp1*^{+/+} and *Sgpp1*^{-/-} mice (supplemental Fig. S2A). *Sgpp1* mRNA was readily detected in *Sgpp1*^{+/+} skin, but it was below the detection limit in *Sgpp1*^{-/-} samples. *Sgpp2* and *Sgpl1* mRNA signals in *Sgpp1*^{+/+} skin were substantially lower than that of *Sgpp1*, suggesting that *Sgpp1* was the most highly expressed of the three S1P degradative enzymes (supplemental Fig. S2A). Compensatory increases of *Sgpp2* or *Sgpl1* mRNA expression were not detected in *Sgpp1*^{-/-} skin (supplemental Fig. S2A). Neither were there significant changes detected in the mRNA levels of the broad specificity LPPs (*Ppap1a*, *Ppap2b*, and *Ppap2c*) (supplemental Fig. S2B).

Skin Barrier Formation in the Absence of *Sgpp1*—We next assessed the development of the epidermal permeability barrier

in *Sgpp1*^{-/-} mice by the ability of their skin to exclude toluidine blue. Normally, the skin permeability barrier begins to form at around embryonic day (E) 16.5, initiating from the dorsal surface and developing ventrally until it is complete by E17.5 (45). Overall, *Sgpp1*^{-/-} embryos displayed a developmental pattern of skin permeability barrier formation indistinguishable from the *Sgpp1*^{+/+} embryos (Fig. 3, A–D). *Sgpp1*^{+/+} and *Sgpp1*^{-/-} early stage E16 embryos stained equally blue, indicating a lack of a permeability barrier at this time (Fig. 3, A and B). However, by late stage E16 both *Sgpp1*^{+/+} and *Sgpp1*^{-/-} embryos largely excluded the blue dye except for the anterior portions of their limbs and snout (Fig. 3, C and D). These results indicate that the skin permeability barrier develops normally in the *Sgpp1*^{-/-} embryos. Three days after birth, *Sgpp1*^{-/-} pups showed normal exclusion of toluidine blue in areas where the skin remained intact (Fig. 3E). However, there was visible dye uptake in desquamated areas, indicating a focally disrupted permeability barrier (Fig. 3E).

Sphingolipid Levels in Epidermis—Sphingolipids were extracted from epidermal sheets obtained from 1- to 2-day-old

Sgpp1 and Keratinocyte Differentiation

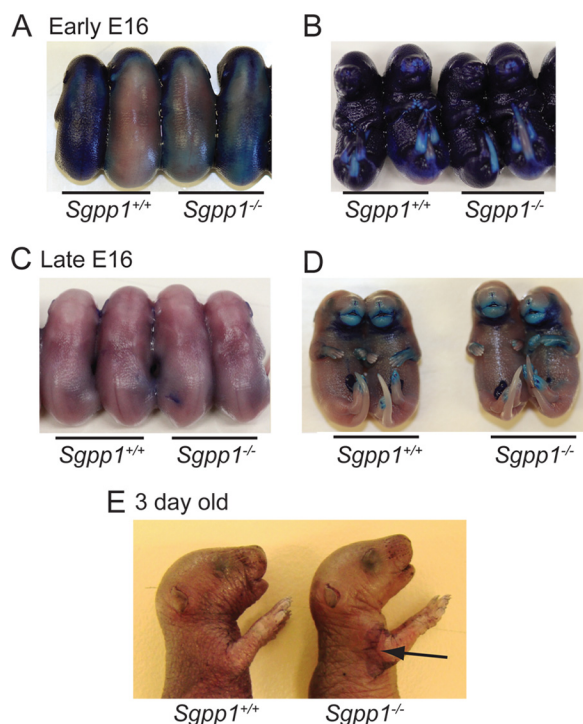


FIGURE 3. Epidermal permeability barrier formation was normal in *Sgpp1*^{-/-} mice. Epidermal barrier acquisition was tested by resistance to toluidine blue staining at early embryonic (E) day E16 (A and B), late day E16 (C and D), and at 3 days after birth (E). Embryos are viewed dorsally (A and C) and ventrally (B and D). In the 3-day-old pups (E), the arrow indicates an area of desquamation that stained with toluidine blue.

Sgpp1^{+/+} and *Sgpp1*^{-/-} mice, and levels of ceramide species, sphingosine, S1P, and dihydro-S1P were determined by mass spectrometry. Total levels of these sphingolipids were not significantly different in *Sgpp1*^{-/-} compared with *Sgpp1*^{+/+} epidermis (Fig. 4, A and B). In addition, total epidermal sphingomyelin levels were not significantly different in *Sgpp1*^{-/-} compared with *Sgpp1*^{+/+} mice (supplemental Fig. S1A). When levels of individual ceramide species were examined, the only significant difference was a decrease in the content of C₂₆-fatty acid-containing ceramide in *Sgpp1*^{-/-} compared with *Sgpp1*^{+/+} epidermis (Fig. 4C).

Abnormal Keratinocyte Proliferation and Differentiation in *Sgpp1*^{-/-} Mice—The thicker epidermal layers observed for *Sgpp1*-deficient skin suggested that increased keratinocyte proliferation was occurring in these mice. To address this possibility, we determined the expression of proliferative markers in skin sections from 2-day-old mice. In *Sgpp1*^{-/-} skin, the expression of the proliferative antigen Ki67 was markedly increased in the stratum basale compared with *Sgpp1*^{+/+} skin, consistent with increased keratinocyte cell division (Fig. 5, A and B). We found highly elevated expression of hyperproliferation-associated keratin 6 (46–48) in *Sgpp1*^{-/-} skin sections throughout the subcorneal epidermal layers (Fig. 5, C and D). Keratin 14, which is expressed in undifferentiated, mitotically active keratinocytes (49), was slightly increased throughout several epidermal layers in *Sgpp1*^{-/-} skin compared with *Sgpp1*^{+/+} skin (Fig. 5, E and F). Significantly increased expression of keratin 14 mRNA in the skin of 2-day-old *Sgpp1* null mice compared with WT mice was confirmed by RT-qPCR

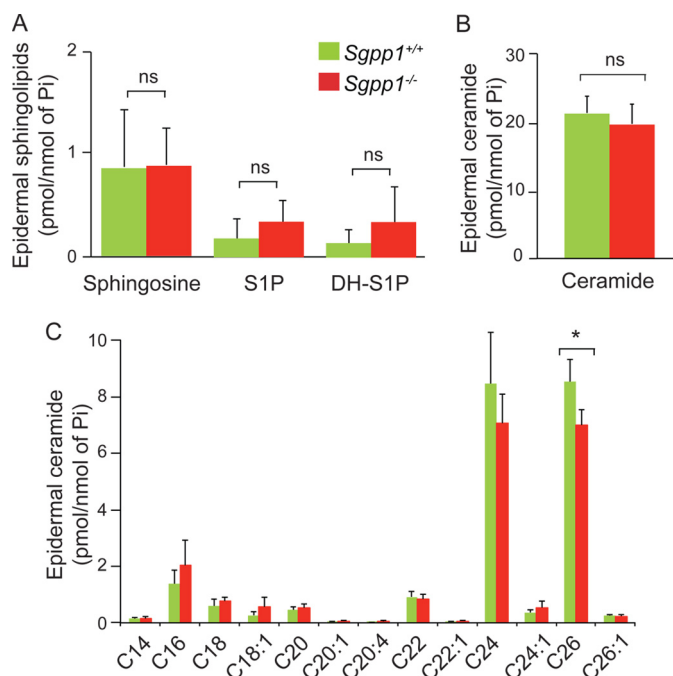


FIGURE 4. Sphingolipid profile in *Sgpp1*^{-/-} mouse epidermis. The sphingolipid profile was determined by HPLC-tandem MS on epidermis isolated from *Sgpp1*^{+/+} and *Sgpp1*^{-/-} 2-day-old pups. Levels of sphingosine, S1P, and dihydro-S1P (A), total ceramide (B), and individual ceramide species with different fatty-acid chain lengths (C) were determined. Values are expressed as picomoles of sphingolipid per nmol of inorganic phosphorous (P_i). Bars represent mean values \pm S.D. $n = 5$ for each genotype. Student's *t* test; *, $p < 0.05$. ns, not significant.

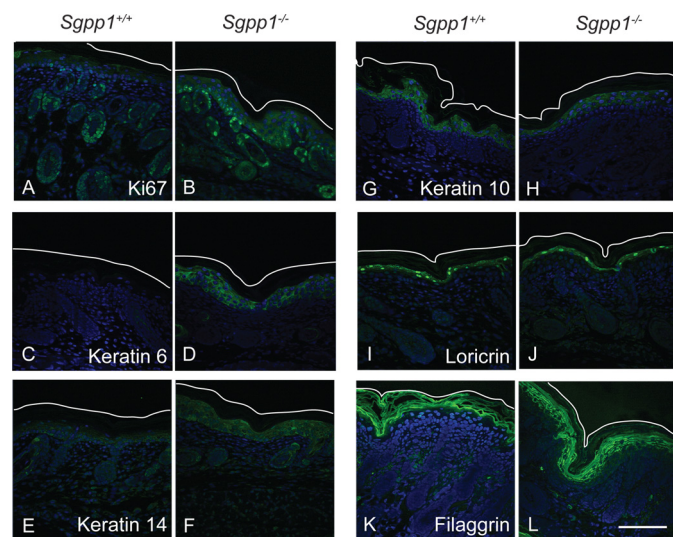


FIGURE 5. Expression of proliferation and keratinocyte differentiation markers are increased in *Sgpp1*^{-/-} skin. Paraffin sections of 2-day-old skin from *Sgpp1*^{+/+} and *Sgpp1*^{-/-} mice were stained with antibodies against Ki67 (A and B), keratin 6 (C and D), keratin 14 (E and F), keratin 10 (G and H), loricrin (I and J), filaggrin (K and L) (green staining), and DAPI (blue). The white line represents the outer edge of the stratum corneum to mark the skin limit on the top of the image. Bar, 100 μ m.

(supplemental Fig. S3A). These results indicate that the deletion of *Sgpp1* leads to epidermal hyperplasia.

We also assessed markers of keratinocyte differentiation in skin sections of *Sgpp1*^{+/+} and *Sgpp1*^{-/-} mice. Expression of keratin 10, a marker of differentiating keratinocytes after growth arrest (50), was expressed similarly in *Sgpp1*^{+/+} and

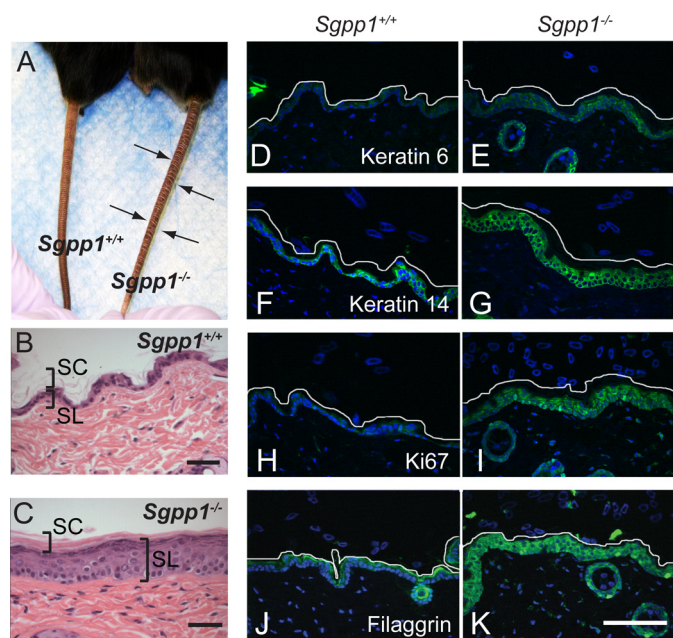


FIGURE 6. Surviving *Sgpp1*^{-/-} adult mice displayed abnormal skin phenotype. A, surviving adult *Sgpp1*^{-/-} mouse and its *Sgpp1*^{+/+} littermate. Arrows indicate the deep constriction rings found on the tails of *Sgpp1*^{-/-} mice. B and C, paraffin sections from *Sgpp1*^{+/+} (B) and *Sgpp1*^{-/-} (C) adult mouse back skin stained with H&E. Bar, 200 μm. SC, stratum corneum; SL, subcorneal layer. D–K, immunohistochemistry of *Sgpp1*^{+/+} and *Sgpp1*^{-/-} adult mouse skin. Paraffin sections were stained with antibodies against keratin 6 (D and E), keratin 14 (F and G), Ki67 antigen (H and I), filaggrin (J and K) (green staining), and DAPI (blue). The white line represents the edge of the stratum corneum to mark the skin limit on the top of the image. Bar, 100 μm.

Sgpp1^{-/-} epidermis (Fig. 5, G and H). Expression of loricrin and filaggrin, two major proteins of the cornified cell envelope in the stratum corneum (51), was also determined. Loricrin expression appeared normal in *Sgpp1*^{-/-} mice (Fig. 5, I and J), although filaggrin expression was expanded into the subcorneal epidermal layers and was relatively weakly expressed in the stratum corneum of the *Sgpp1*^{-/-} mice (Fig. 5, K and L). We also quantified the expression of these differentiation-related genes by RT-qPCR. We found that mRNA expression of keratin 10 and loricrin was not significantly different between *Sgpp1*^{+/+} and *Sgpp1*^{-/-} skin, although filaggrin mRNA levels were significantly increased in *Sgpp1*^{-/-} skin compared with skin from WT mice (supplemental Fig. S3, B–D). Together, these results show that the epidermis of the *Sgpp1*^{-/-} mice exhibits abnormalities both in keratinocyte differentiation and proliferation.

Adult *Sgpp1*^{-/-} Mice Have an Ichthyosis-like Phenotype—The rare surviving adult *Sgpp1*^{-/-} mice were similar to *Sgpp1*^{+/+} mice in size (data not shown). However, the skin on their tails had an ichthyotic appearance (Fig. 6A). Histological analysis of dorsal skin (Fig. 6, B and C) from adult *Sgpp1*^{+/+} and *Sgpp1*^{-/-} mice revealed that, as in the newborns, the *Sgpp1*^{-/-} epidermis was significantly thicker than that from *Sgpp1*^{+/+} mice. The stratum corneum appeared dense and compact (Fig. 6C).

Expression of keratin 6 (Fig. 6, D and E), keratin 14 (Fig. 6, F and G), and Ki67 antigen (Fig. 6, H and I) was elevated in sub-cortical layers of the *Sgpp1*^{-/-} epidermis from adult mice, consistent with epidermal hyperplasia. In *Sgpp1*^{-/-} epidermis,

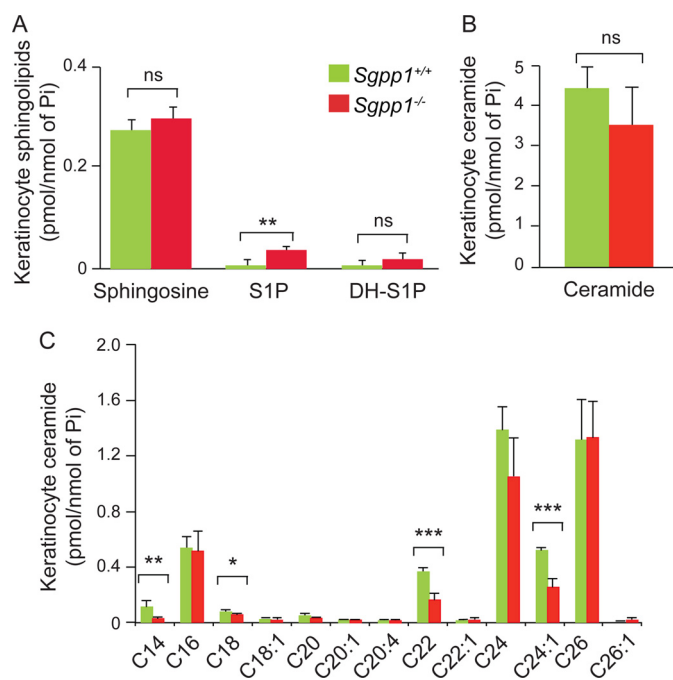


FIGURE 7. Sphingolipid profile of *Sgpp1*^{-/-} keratinocytes. Primary keratinocytes from skin of 1-day-old *Sgpp1*^{+/+} and *Sgpp1*^{-/-} mice were grown in low Ca²⁺ media for 3–4 days. The sphingolipid profile of each culture was determined by HPLC-tandem MS. Levels of sphingosine, S1P, and dihydro-S1P (A), total ceramide (B), and individual ceramide fatty acid chain species (C) were determined. Values are expressed as picomoles of sphingolipid per nmol of inorganic phosphorous (P). Bars represent mean values ± S.D. n = 5 for each genotype. Student's t test; *, p < 0.05; **, p < 0.01; ***, p < 0.001. ns, not significant.

filaggrin expression was highly elevated and extended into deeper epidermal layers (Fig. 6, J and K) compared with *Sgpp1*^{+/+} epidermis.

We quantified S1P levels in *Sgpp1*^{+/+} and *Sgpp1*^{-/-} plasma, and we found no significant difference (supplemental Fig. S4).

***Sgpp1* Deletion Increases S1P Levels and Alters the Gene Expression Profile of Keratinocytes in Vitro—**Because it was possible that the keratinocyte abnormalities observed in the *Sgpp1*^{-/-} mice might be the result of extrinsic factors, such as an altered stratum corneum or an effect of the *Sgpp1* deletion on other skin cell types, we wanted to determine whether the effect of the *Sgpp1* deletion was intrinsic to keratinocytes. To investigate this, we isolated and grew keratinocytes from *Sgpp1*^{+/+} and *Sgpp1*^{-/-} mice under low Ca²⁺ conditions, which impede differentiation, for 3–4 days (39).

We first determined the sphingolipid profile of cultured keratinocytes by HPLC-tandem MS. We found that the S1P levels in the *Sgpp1*^{-/-} keratinocytes were significantly increased compared with *Sgpp1*^{+/+} mice, although dihydro-S1P and sphingosine levels (Fig. 7A) as well as sphingomyelin levels (supplemental Fig. S1B) were unchanged. Although total ceramide levels were similar in keratinocytes from *Sgpp1*^{+/+} and *Sgpp1*^{-/-} mice (Fig. 7B), the ceramide species containing fatty acid lengths of C₁₄, C₁₈, C₂₂, and C_{24:1} in *Sgpp1*^{-/-} keratinocytes were all significantly decreased compared with *Sgpp1*^{+/+} keratinocytes (Fig. 7C).

We next performed gene expression profiling on mRNA from cultured keratinocytes from *Sgpp1*^{+/+} and *Sgpp1*^{-/-} mice using Affymetrix GeneChip Mouse Genome 430 2.0

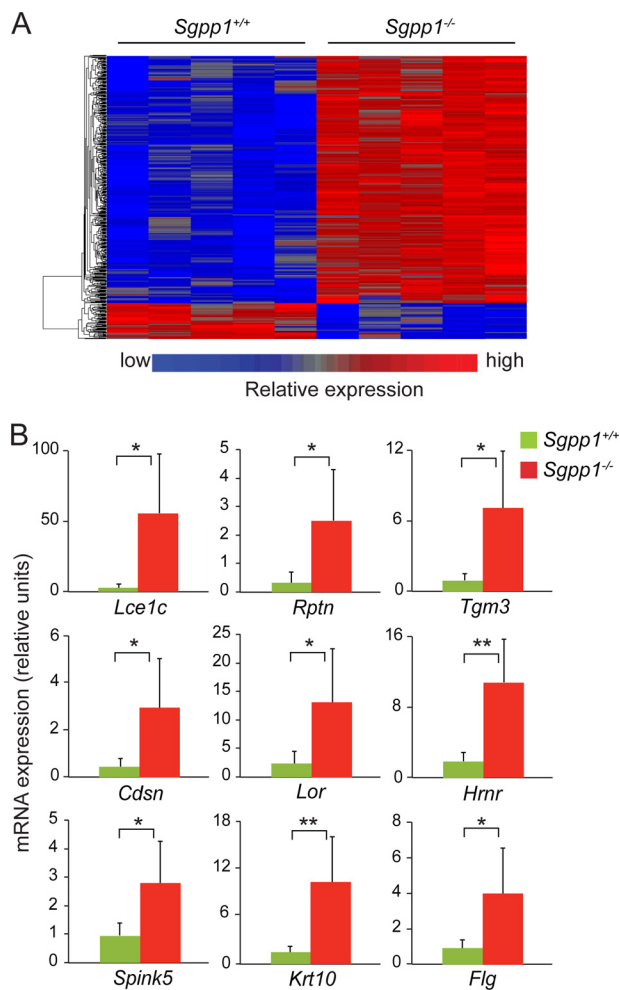


FIGURE 8. Gene expression profile of keratinocytes in vitro. A, microarray gene expression analysis was performed with RNA from five *Sgpp1*^{+/+} and five *Sgpp1*^{-/-} keratinocyte cultures, isolated from individual mice, grown in low Ca²⁺ media for 3–4 days. The heat map shows the raw signal values of genes that are significantly different between *Sgpp1*^{+/+} and *Sgpp1*^{-/-} groups, using a cutoff of $p < 0.05$ and a fold change of greater than 2. B, expression levels of nine genes among the top 50 determined by microarray analysis to be overexpressed in *Sgpp1*^{-/-} keratinocytes were validated by RT-qPCR. Results are expressed as mean value \pm S.D. $n = 6$ for both genotypes. Student's *t* test; *, $p < 0.05$; **, $p < 0.01$.

arrays. From the microarray data, we identified more than 700 gene annotated probe sets that showed significant changes between keratinocytes from *Sgpp1*^{+/+} and *Sgpp1*^{-/-} mice, using a cutoff of $p < 0.05$ and a fold change of greater than 2 (Fig. 8A). Examination of the top genes that were significantly overexpressed in the *Sgpp1*^{-/-} keratinocytes revealed that many of them were associated with keratinocyte differentiation (Fig. 8B and supplemental Table 1). These included several genes of the late cornified envelope family (51) (Fig. 8B and supplemental Table 1). Indeed, the Gene Ontology categories “keratinization” (1.8-fold; $p < 3.2\text{E-}09$) and “cornified envelope” (2.7-fold; $p < 6.7\text{E-}10$) were significantly elevated in *Sgpp1*^{-/-} keratinocytes when compared with *Sgpp1*^{+/+} keratinocytes (supplemental Fig. S5, A and B). These results indicate that the deletion of *Sgpp1* has an intrinsic effect on keratinocytes that causes an elevated expression of genes associated with their differentiation.

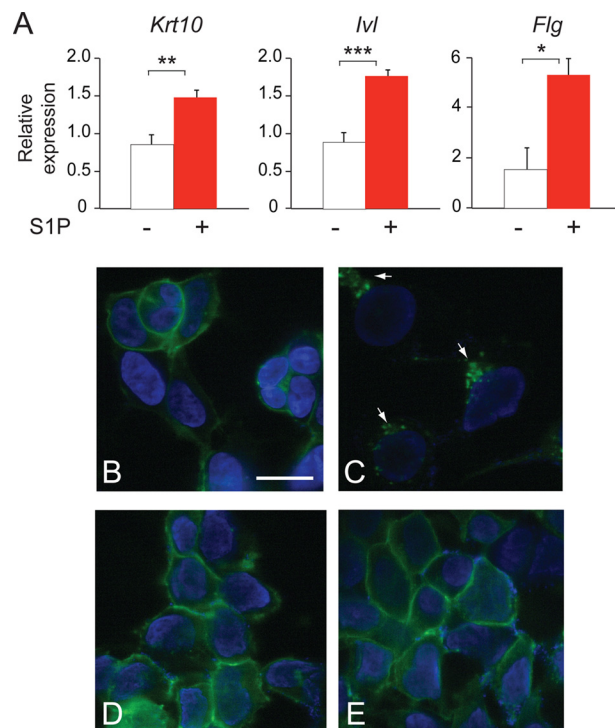


FIGURE 9. Role of S1P in keratinocyte differentiation. A, mouse keratinocytes were incubated with 10^{-7} M S1P for 2 days, and gene expression was determined by RT-qPCR. Data are expressed as mean value \pm S.D., $n = 3$ for each phenotype, and is representative of three independent experiments. Student's *t* test; *, $p < 0.05$; **, $p < 0.01$; ***, $p < 0.001$. B–E, S1PR1-GFP receptor-expressing HEK293 cells were incubated for 60 min with C-DMEM (B), 10^{-7} M S1P (C), *Sgpp1*^{+/+} conditioned medium (D), and *Sgpp1*^{-/-} conditioned medium (E). Cells were then fixed and examined using a Zeiss confocal laser scanning microscope under a $\times 63$ oil objective. Bar, 20 μm .

Treatment of WT keratinocytes with 10^{-7} M S1P also led to an increase in the expression of the differentiation-related genes keratin 10, involucrin, and filaggrin (Fig. 9A). This result indicates that elevating S1P levels is able to recapitulate the enhanced differentiation observed in *Sgpp1* null keratinocytes and points to elevated S1P levels generated by the *Sgpp1* deletion as responsible for the accelerated differentiation phenotype.

To further characterize the mechanism through which S1P regulates keratinocyte differentiation, we studied whether S1P was acting “outside-in” (52) by ligation of S1P receptors. We determined if there was sufficient S1P released by keratinocytes to induce internalization of a S1PR1-GFP chimeric receptor expressed on the plasma membrane of HEK293 cells (44). Addition of 10^{-7} M S1P completely induced internalization of the receptor from the plasma membrane to perinuclear vesicles as reported (44) (Fig. 9, B and C). However, after the addition of 5-day conditioned medium from *Sgpp1*^{+/+} or *Sgpp1*^{-/-} keratinocytes, the S1PR1-GFP receptor remained at the plasma membrane (Fig. 9, D and E). The results show that there is insufficient S1P in keratinocyte cultures to induce S1PR1-GFP internalization, a surrogate for receptor activation.

Sgpp1 Deletion Increases Ca²⁺ Levels within the Epidermis—S1P has been shown to induce differentiation in keratinocytes by controlling intracellular Ca²⁺ levels (6, 32, 33, 34, 53). To determine whether epidermal Ca²⁺ was increased *in vivo* by the *Sgpp1* deletion, Calcium Green-1, which exhibits a fluores-

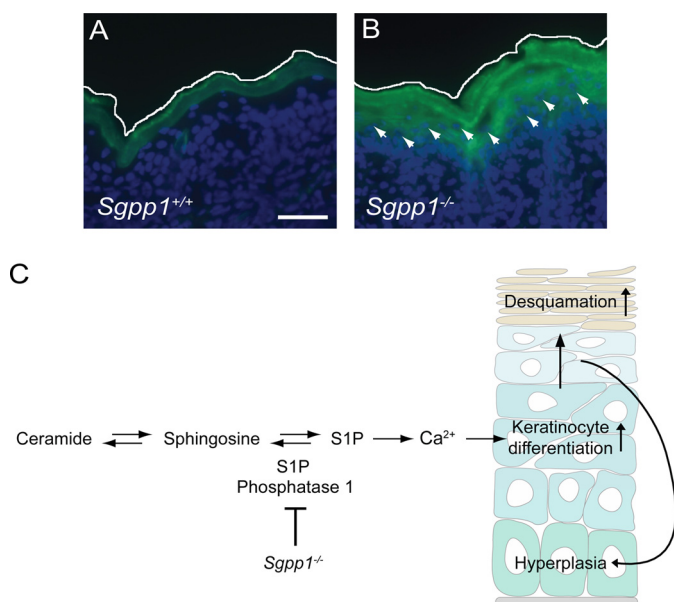


FIGURE 10. Mechanism for the skin phenotype found in *Sgpp1*^{-/-} mice. A and B, Ca^{2+} distribution was visualized *in situ* by Calcium Green-1 staining on frozen skin sections from *Sgpp1*^{+/+} (A) and *Sgpp1*^{-/-} (B) pups. Arrows indicate staining of nucleated cells in the *Sgpp1*^{-/-} sections. The white line represents the outer edge of the stratum corneum to mark the skin limit on the top of the image. Bar, 100 μm . B and C, proposed mechanism. The S1P phosphatase encoded by *Sgpp1* is relatively highly expressed in differentiating keratinocytes. Its deletion in keratinocytes raises S1P levels, triggering Ca^{2+} -induced keratinocyte differentiation, resulting in a compensatory increase in keratinocyte proliferation leading to increased desquamation.

cence intensity increase upon binding Ca^{2+} , was used to detect Ca^{2+} in skin sections. *Sgpp1*^{+/+} skin showed fluorescence largely confined to the outer epidermal layers as described (Fig. 10A) (33, 54, 55). In contrast, *Sgpp1*^{-/-} skin displayed higher fluorescence that extended well into the nucleated layers of the epidermis (Fig. 10B). This result indicates that the *Sgpp1* deletion increases Ca^{2+} levels within epidermis.

DISCUSSION

Here, we have demonstrated a novel role for *Sgpp1* in the regulation of epidermal homeostasis. Mice with an inactive *Sgpp1* gene developed an ichthyosis-like phenotype, characterized by desquamation, epidermal hyperplasia, and abnormal expression of keratinocyte differentiation markers. Focally severe desquamation began a few days after birth and is a possible cause of the demise of most of the *Sgpp1*^{-/-} mice. Those *Sgpp1*^{-/-} mice that survived developed ichthyotic skin that was evident on their tails. Other than the skin-related phenotype, adult *Sgpp1*^{-/-} mice appeared grossly normal.

The lack of any other apparent major phenotypic consequences may be due to alternative pathways that serve to maintain low S1P levels in most tissue compartments. A major S1P degradative pathway is via S1P lyase-mediated cleavage, a process that occurs in many cells and tissues (56). S1P lyase-deficient mice exhibit highly elevated S1P levels in circulation and in tissues, along with diverse phenotypic aberrations, notably in the immune system (9, 57), but, interestingly, not the skin phenotype exhibited by the *Sgpp1* null mice. The phenotypic expression of a defect within the epidermis in the *Sgpp1*^{-/-} mice suggests that *Sgpp1* might serve a unique function within differentiating keratinocytes.

As keratinocytes differentiate within the epidermis, they synthesize and package complex sphingolipids, such as sphingomyelin and β -glucosylceramide, along with other lipids, into lamellar bodies that are secreted by cells of the outer layers in the stratum granulosum (28). These complex sphingolipids in the lamellar bodies are then processed in the extracellular space into ceramides. Epidermal ceramides are critical for barrier function, accounting for 30–40% of the lipids in the stratum corneum (27, 58–60). The acquisition of a normal skin permeability barrier during embryonic development in the *Sgpp1* null mice indicated that the sphingolipid metabolic pathway for the production of extracellular ceramides of the stratum corneum was not adversely impacted by the deletion of *Sgpp1*. Consistent with the acquisition of a normal permeability barrier were the normal ceramide and sphingomyelin levels in *Sgpp1*^{-/-} skin.

Our results point to an intrinsic defect in the *Sgpp1*^{-/-} keratinocytes as a mechanism to account for the abnormal epidermal phenotype in these mice (Fig. 10C). This conclusion is supported by the microarray analysis showing that *Sgpp1*^{-/-} keratinocytes exhibit a gene expression profile distinct from WT keratinocytes, in which genes associated with keratinocyte differentiation and cornified envelope formation were significantly elevated. An intrinsic cellular defect resulting in accelerated keratinocyte differentiation would be consistent with the epidermal skin phenotype of the *Sgpp1*^{-/-} mice, characterized by elevated keratinocyte differentiation markers, such as filaggrin and keratin 10. The keratinocyte hyperplasia in the *Sgpp1* null epidermis may be explained as a secondary compensatory effect due to increased differentiation (Fig. 10C). The heightened keratinocyte growth and differentiation could then lead to the abnormal desquamation seen in the pups and the ichthyotic condition observed in the adult mice. Although accumulation of S1P was not found in the whole *Sgpp1*^{-/-} epidermis, a severalfold increase in cellular S1P was detected in cultured *Sgpp1*^{-/-} keratinocytes, which is consistent with increased intracellular levels of S1P as the cause of the keratinocyte defects (Fig. 10C). Moreover, S1P addition to WT keratinocytes enhanced their differentiation, as has been described (6, 32, 33, 53), further implicating S1P elevation in keratinocytes as the cause of the *Sgpp1*^{-/-} epidermal phenotype.

S1P has been reported to induce Ca^{2+} signaling, a key process for epidermal and keratinocyte differentiation (5, 6, 31). The regulated release of Ca^{2+} from ER and Golgi stores, as well as the Ca^{2+} influx through Ca^{2+} -permeable ion channels, induces the transcription of genes associated with keratinocyte differentiation, such as keratin 1 and 10, filaggrin, and loricrin (61). S1P has long been known to induce elevations of intracellular Ca^{2+} levels through the release from internal stores (5, 6), and its metabolism is believed to serve as a complementary Ca^{2+} signaling pathway to promote keratinocyte differentiation (31). Elevating S1P levels through sphingosine kinase activation or lowering S1P lyase levels has been shown to increase Ca^{2+} levels and promote differentiation (33, 34). Furthermore, the up-regulation of alkaline and acid ceramidases (see scheme in Fig. 1A) to increase sphingosine and S1P production mediates Ca^{2+} -induced keratinocyte differentiation (62). The *Sgpp1* deletion caused a striking elevation of Ca^{2+} indicator staining within the epidermis consistent with an abnormally enhanced

Ca²⁺ response inducing the differentiation of keratinocytes. S1P exerts functional effects on keratinocytes through both direct intracellular and extracellular receptor-mediated signaling pathways (6). Our results are most consistent with an intracellular mechanism of S1P-induced differentiation, rather than an extracellular receptor-mediated effect, because we could not detect extracellular, bioactive S1P secreted by *Sgpp1*^{−/−} keratinocytes.

The expression of *Sgpp1* on the differentiating layers of the epithelium supports the notion that SPP1 activity may be important in controlling S1P levels as keratinocytes differentiate within the skin. Overall, the results are consistent with the possibility that the activation of sphingolipid metabolism signals keratinocytes to differentiate via the attendant production of bioactive S1P. *De novo* sphingolipid synthesis in epidermis is up-regulated after epidermal damage (63). One function of this increased *de novo* synthesis after injury is believed to be for the replenishment of barrier lipids. Another may be to provide a lipid signal, via S1P, to promote a keratinocyte-differentiation program.

The functions of the SPPs, in a physiological context, have been enigmatic. Here, we have defined a novel functional role for SPP1 in keratinocyte differentiation and in skin biology. The importance of SPP1 in keratinocytes may identify a key role for S1P metabolism and signaling in their function and may suggest therapeutic avenues for skin diseases with defects in keratinocyte differentiation.

Acknowledgment—We thank Maria Irene Morasso for useful discussions and for providing reagents.

REFERENCES

- Rivera, J., Proia, R. L., and Olivera, A. (2008) The alliance of sphingosine 1-phosphate and its receptors in immunity. *Nat. Rev. Immunol.* **8**, 753–763
- Fyrst, H., and Saba, J. D. (2010) An update on sphingosine 1-phosphate and other sphingolipid mediators. *Nat. Chem. Biol.* **6**, 489–497
- Maceyka, M., Harikumar, K. B., Milstien, S., and Spiegel, S. (2012) Sphingosine 1-phosphate signaling and its role in disease. *Trends Cell Biol.* **22**, 50–60
- Hannun, Y. A., and Obeid, L. M. (2008) Principles of bioactive lipid signalling: lessons from sphingolipids. *Nat. Rev. Mol. Cell Biol.* **9**, 139–150
- Spiegel, S., and Milstien, S. (2003) Sphingosine 1-phosphate: an enigmatic signalling lipid. *Nat. Rev. Mol. Cell Biol.* **4**, 397–407
- Meyer Zu Heringdorf, D. (2004) Lysophospholipid receptor-dependent and -independent calcium signaling. *J. Cell Biochem.* **92**, 937–948
- Alvarez, S. E., Harikumar, K. B., Hait, N. C., Allegood, J., Strub, G. M., Kim, E. Y., Maceyka, M., Jiang, H., Luo, C., Kordula, T., Milstien, S., and Spiegel, S. (2010) Sphingosine 1-phosphate is a missing cofactor for the E3 ubiquitin ligase TRAF2. *Nature* **465**, 1084–1088
- Hait, N. C., Allegood, J., Maceyka, M., Strub, G. M., Harikumar, K. B., Singh, S. K., Luo, C., Marmorstein, R., Kordula, T., Milstien, S., and Spiegel, S. (2009) Regulation of histone acetylation in the nucleus by sphingosine 1-phosphate. *Science* **325**, 1254–1257
- Bektas, M., Allende, M. L., Lee, B. G., Chen, W., Amar, M. J., Remaley, A. T., Saba, J. D., and Proia, R. L. (2010) Sphingosine-1-phosphate lyase deficiency disrupts lipid homeostasis in liver. *J. Biol. Chem.* **285**, 10880–10889
- Merrill, A. H., Jr. (2011) Sphingolipid and glycosphingolipid metabolic pathways in the era of sphingolipidomics. *Chem. Rev.* **111**, 6387–6422
- Pyne, S., Long, J. S., Ktistakis, N. T., and Pyne, N. J. (2005) Lipid phosphate phosphatases and lipid phosphate signalling. *Biochem. Soc. Trans.* **33**, 1370–1374
- Le Stunff, H., Peterson, C., Liu, H., Milstien, S., and Spiegel, S. (2002) Sphingosine-1-phosphate and lipid phosphohydrolases. *Biochim. Biophys. Acta* **1582**, 8–17
- Sciorra, V. A., and Morris, A. J. (2002) Roles for lipid phosphate phosphatases in regulation of cellular signaling. *Biochim. Biophys. Acta* **1582**, 45–51
- Brindley, D. N., and Pilquill, C. (2009) Lipid phosphate phosphatases and signaling. *J. Lipid Res.* **50**, S225–S230
- Mandala, S. M., Thornton, R., Galve-Roperh, I., Poulton, S., Peterson, C., Olivera, A., Bergstrom, J., Kurtz, M. B., and Spiegel, S. (2000) Molecular cloning and characterization of a lipid phosphohydrolase that degrades sphingosine 1-phosphate and induces cell death. *Proc. Natl. Acad. Sci. U.S.A.* **97**, 7859–7864
- Mao, C., Wadleigh, M., Jenkins, G. M., Hannun, Y. A., and Obeid, L. M. (1997) Identification and characterization of *Saccharomyces cerevisiae* dihydrosphingosine-1-phosphate phosphatase. *J. Biol. Chem.* **272**, 28690–28694
- Mandala, S. M., Thornton, R., Tu, Z., Kurtz, M. B., Nickels, J., Broach, J., Menzeleev, R., and Spiegel, S. (1998) Sphingoid base 1-phosphate phosphatase: a key regulator of sphingolipid metabolism and stress response. *Proc. Natl. Acad. Sci. U.S.A.* **95**, 150–155
- Le Stunff, H., Peterson, C., Thornton, R., Milstien, S., Mandala, S. M., and Spiegel, S. (2002) Characterization of murine sphingosine-1-phosphate phosphohydrolase. *J. Biol. Chem.* **277**, 8920–8927
- Ogawa, C., Kihara, A., Gokoh, M., and Igarashi, Y. (2003) Identification and characterization of a novel human sphingosine-1-phosphate phosphohydrolase, hsp26. *J. Biol. Chem.* **278**, 1268–1272
- Breard, B., Ramos-Perez, W. D., Mendoza, A., Salous, A. K., Gobert, M., Huang, Y., Adams, R. H., Lafaille, J. J., Escalante-Alcalde, D., Morris, A. J., and Schwab, S. R. (2011) Lipid phosphate phosphatase 3 enables efficient thymic egress. *J. Exp. Med.* **208**, 1267–1278
- Giussani, P., Maceyka, M., Le Stunff, H., Mikami, A., Lépine, S., Wang, E., Kelly, S., Merrill, A. H., Jr., Milstien, S., and Spiegel, S. (2006) Sphingosine-1-phosphate phosphohydrolase regulates endoplasmic reticulum-to-Golgi trafficking of ceramide. *Mol. Cell. Biol.* **26**, 5055–5069
- Lépine, S., Allegood, J. C., Edmonds, Y., Milstien, S., and Spiegel, S. (2011) Autophagy induced by deficiency of sphingosine-1-phosphate phosphohydrolase 1 is switched to apoptosis by calpain-mediated autophagy-related gene 5 (Atg5) cleavage. *J. Biol. Chem.* **286**, 44380–44390
- Lépine, S., Allegood, J. C., Park, M., Dent, P., Milstien, S., and Spiegel, S. (2011) Sphingosine-1-phosphate phosphohydrolase-1 regulates ER stress-induced autophagy. *Cell Death Differ.* **18**, 350–361
- Peter, B. F., Lidington, D., Harada, A., Bolz, H. J., Vogel, L., Heximer, S., Spiegel, S., Pohl, U., and Bolz, S. S. (2008) Role of sphingosine-1-phosphate phosphohydrolase 1 in the regulation of resistance artery tone. *Circ. Res.* **103**, 315–324
- Le Stunff, H., Mikami, A., Giussani, P., Hobson, J. P., Jolly, P. S., Milstien, S., and Spiegel, S. (2004) Role of sphingosine-1-phosphate phosphatase 1 in epidermal growth factor-induced chemotaxis. *J. Biol. Chem.* **279**, 34290–34297
- Mechtcheriakova, D., Wlachs, A., Sobanov, J., Kopp, T., Reuschel, R., Bornancin, F., Cai, R., Zemmann, B., Urtz, N., Stingl, G., Zlabinger, G., Woisetschlager, M., Baumruker, T., and Billich, A. (2007) Sphingosine 1-phosphate phosphatase 2 is induced during inflammatory responses. *Cell. Signal.* **19**, 748–760
- Feingold, K. R. (2009) The outer frontier: the importance of lipid metabolism in the skin. *J. Lipid Res.* **50**, S417–S422
- Holleran, W. M., Takagi, Y., and Uchida, Y. (2006) Epidermal sphingolipids: metabolism, function, and roles in skin disorders. *FEBS Lett.* **580**, 5456–5466
- Elias, P. M., and Feingold, K. R. (1992) Lipids and the epidermal water barrier: metabolism, regulation, and pathophysiology. *Semin. Dermatol.* **11**, 176–182
- Schuetz, C. G., Pierstorff, B., Huettler, S., and Sandhoff, K. (2001) Sphingolipid activator proteins: proteins with complex functions in lipid degradation and skin biogenesis. *Glycobiology* **11**, 81R–90R
- Herzinger, T., Kleuser, B., Schäfer-Korting, M., and Korting, H. C. (2007)

- Sphingosine 1-phosphate signaling and the skin. *Am. J. Clin. Dermatol.* **8**, 329–336
32. Vogler, R., Sauer, B., Kim, D. S., Schäfer-Korting, M., and Kleuser, B. (2003) Sphingosine 1-phosphate and its potentially paradoxical effects on critical parameters of cutaneous wound healing. *J. Invest. Dermatol.* **120**, 693–700
33. Hong, J. H., Youm, J. K., Kwon, M. J., Park, B. D., Lee, Y. M., Lee, S. I., Shin, D. M., and Lee, S. H. (2008) K6PC-5, a direct activator of sphingosine kinase 1, promotes epidermal differentiation through intracellular Ca^{2+} signaling. *J. Invest. Dermatol.* **128**, 2166–2178
34. Celli, A., Mackenzie, D. S., Zhai, Y., Tu, C. L., Bikle, D. D., Holleran, W. M., Uchida, Y., and Mauro, T. M. (2012) SERCA2-controlled Ca^{2+} -dependent keratinocyte adhesion and differentiation is mediated via the sphingolipid pathway: a therapeutic target for Darier's disease. *J. Invest. Dermatol.* **132**, 1188–1195
35. Kim, D. S., Kim, S. Y., Kleuser, B., Schäfer-Korting, M., Kim, K. H., and Park, K. C. (2004) Sphingosine 1-phosphate inhibits human keratinocyte proliferation via Akt/protein kinase B inactivation. *Cell. Signal.* **16**, 89–95
36. Schmitz, E. I., Potteck, H., Schuppel, M., Manggau, M., Wahyidin, E., and Kleuser, B. (2012) Sphingosine 1-phosphate protects primary human keratinocytes from apoptosis via nitric oxide formation through the receptor subtype S1P(3). *Mol. Cell. Biochem.* **371**, 165–176
37. Liu, Y., Wada, R., Yamashita, T., Mi, Y., Deng, C. X., Hobson, J. P., Rosenfeldt, H. M., Nava, V. E., Chae, S. S., Lee, M. J., Liu, C. H., Hla, T., Spiegel, S., and Proia, R. L. (2000) Edg-1, the G protein-coupled receptor for sphingosine-1-phosphate, is essential for vascular maturation. *J. Clin. Invest.* **106**, 951–961
38. Denda, M., Hosoi, J., and Asida, Y. (2000) Visual imaging of ion distribution in human epidermis. *Biochem. Biophys. Res. Commun.* **272**, 134–137
39. Lichti, U., Anders, J., and Yuspa, S. H. (2008) Isolation and short-term culture of primary keratinocytes, hair follicle populations, and dermal cells from newborn mice and keratinocytes from adult mice for *in vitro* analysis and for grafting to immunodeficient mice. *Nat. Protoc.* **3**, 799–810
40. Hwang, J., Kita, R., Kwon, H. S., Choi, E. H., Lee, S. H., Udey, M. C., and Morasso, M. I. (2011) Epidermal ablation of Dlx3 is linked to IL-17-associated skin inflammation. *Proc. Natl. Acad. Sci. U.S.A.* **108**, 11566–11571
41. Vasireddy, V., Uchida, Y., Salem, N., Jr., Kim, S. Y., Mandal, M. N., Reddy, G. B., Bodepudi, R., Alderson, N. L., Brown, J. C., Hama, H., Dlugosz, A., Elias, P. M., Holleran, W. M., and Ayyagari, R. (2007) Loss of functional ELOVL4 depletes very long-chain fatty acids ($> \text{or} = \text{C}28$) and the unique ω -O-acylceramides in skin leading to neonatal death. *Hum. Mol. Genet.* **16**, 471–482
42. Bielawski, J., Szulc, Z. M., Hannun, Y. A., and Bielawska, A. (2006) Simultaneous quantitative analysis of bioactive sphingolipids by high-performance liquid chromatography-tandem mass spectrometry. *Methods* **39**, 82–91
43. Saitoh, M., Sakakihara, Y., Mizuguchi, M., Itoh, M., Takashima, S., Iwamori, M., Kamoshita, S., and Igarashi, T. (2007) Increase of ceramide monohexoside and dipalmitoylglycerophospholipids in the brain of Zellweger syndrome. *Neurosci. Lett.* **417**, 165–170
44. Liu, C. H., Thangada, S., Lee, M. J., Van Brocklyn, J. R., Spiegel, S., and Hla, T. (1999) Ligand-induced trafficking of the sphingosine 1-phosphate receptor EDG-1. *Mol. Biol. Cell* **10**, 1179–1190
45. Hardman, M. J., Sisi, P., Banbury, D. N., and Byrne, C. (1998) Patterned acquisition of skin barrier function during development. *Development* **125**, 1541–1552
46. Weiss, R. A., Eichner, R., and Sun, T. T. (1984) Monoclonal antibody analysis of keratin expression in epidermal diseases: a 48- and 56-kilodalton keratin as molecular markers for hyperproliferative keratinocytes. *J. Cell Biol.* **98**, 1397–1406
47. Mansbridge, J. N., and Knapp, A. M. (1987) Changes in keratinocyte maturation during wound healing. *J. Invest. Dermatol.* **89**, 253–263
48. Stoler, A., Kopan, R., Duvic, M., and Fuchs, E. (1988) Use of monospecific antisera and cRNA probes to localize the major changes in keratin expression during normal and abnormal epidermal differentiation. *J. Cell Biol.* **107**, 427–446
49. Fuchs, E., and Cleveland, D. W. (1998) A structural scaffolding of intermediate filaments in health and disease. *Science* **279**, 514–519
50. Fuchs, E., and Green, H. (1980) Changes in keratin gene expression during terminal differentiation of the keratinocyte. *Cell* **19**, 1033–1042
51. Candi, E., Schmidt, R., and Melino, G. (2005) The cornified envelope: a model of cell death in the skin. *Nat. Rev. Mol. Cell Biol.* **6**, 328–340
52. Spiegel, S., and Milstien, S. (2000) Sphingosine 1-phosphate: signaling inside and out. *FEBS Lett.* **476**, 55–57
53. Kwon, Y. B., Kim, C. D., Youm, J. K., Gwak, H. S., Park, B. D., Lee, S. H., Jeon, S., Kim, B. J., Seo, Y. J., Park, J. K., and Lee, J. H. (2007) Novel synthetic ceramide derivatives increase intracellular calcium levels and promote epidermal keratinocyte differentiation. *J. Lipid Res.* **48**, 1936–1943
54. Menon, G. K., Grayson, S., and Elias, P. M. (1985) Ionic calcium reservoirs in mammalian epidermis: ultrastructural localization by ion-capture cytochemistry. *J. Invest. Dermatol.* **84**, 508–512
55. Elias, P. M., Nau, P., Hanley, K., Cullander, C., Crumrine, D., Bench, G., Sideras-Haddad, E., Mauro, T., Williams, M. L., and Feingold, K. R. (1998) Formation of the epidermal calcium gradient coincides with key milestones of barrier ontogenesis in the rodent. *J. Invest. Dermatol.* **110**, 399–404
56. Olivera, A., Allende, M. L., and Proia, R. L. (2013) Shaping the landscape: Metabolic regulation of S1P gradients. *Biochim. Biophys. Acta* **183**, 193–202
57. Allende, M. L., Bektas, M., Lee, B. G., Bonifacio, E., Kang, J., Tuymetova, G., Chen, W., Saba, J. D., and Proia, R. L. (2011) Sphingosine-1-phosphate lyase deficiency produces a pro-inflammatory response while impairing neutrophil trafficking. *J. Biol. Chem.* **286**, 7348–7358
58. Holleran, W. M., Man, M. Q., Gao, W. N., Menon, G. K., Elias, P. M., and Feingold, K. R. (1991) Sphingolipids are required for mammalian epidermal barrier function. Inhibition of sphingolipid synthesis delays barrier recovery after acute perturbation. *J. Clin. Invest.* **88**, 1338–1345
59. Elias, P. M., and Menon, G. K. (1991) Structural and lipid biochemical correlates of the epidermal permeability barrier. *Adv. Lipid Res.* **24**, 1–26
60. Uchida, Y., and Holleran, W. M. (2008) ω -O-Acylceramide, a lipid essential for mammalian survival. *J. Dermatol. Sci.* **51**, 77–87
61. Li, L., Tucker, R. W., Hennings, H., and Yuspa, S. H. (1995) Chelation of intracellular Ca^{2+} inhibits murine keratinocyte differentiation *in vitro*. *J. Cell Physiol.* **163**, 105–114
62. Sun, W., Xu, R., Hu, W., Jin, J., Crellin, H. A., Bielawski, J., Szulc, Z. M., Thiers, B. H., Obeid, L. M., and Mao, C. (2008) Up-regulation of the human alkaline ceramidase 1 and acid ceramidase mediates calcium-induced differentiation of epidermal keratinocytes. *J. Invest. Dermatol.* **128**, 389–397
63. Harris, I. R., Farrell, A. M., Grunfeld, C., Holleran, W. M., Elias, P. M., and Feingold, K. R. (1997) Permeability barrier disruption coordinately regulates mRNA levels for key enzymes of cholesterol, fatty acid, and ceramide synthesis in the epidermis. *J. Invest. Dermatol.* **109**, 783–787